Toosendanin induces apoptosis of MKN-45 human gastric cancer cells partly through miR-23a-3p-mediated downregulation of *BCL2*

SHULI SHAO[1,2], SHANSHAN LI[1], CHANG LIU[1], WEIWEI ZHANG[1,2], ZHENZHU ZHANG[1,2], SHAOWEI ZHU[1], YUNJIANAN FENG[1] and YANG PAN[1]

[1]Department of Life Science and Agroforestry; [2]Key Laboratory of Resistance Gene Engineering and Protection of Biodiversity in Cold Areas, Qiqihar University, Qiqihar, Heilongjiang 161006, P.R. China

Received August 7, 2019; Accepted May 22, 2020

DOI: 10.3892/mmr.2020.11263

Abstract. Toosendanin (TSN) is a tetracyclic triterpenoid extracted from *Melia toosendan* Sieb, et Zucc, which primarily grows in specific areas of China. Although toosendanin (TSN) exerts antitumoral effects on various human cancer cells, its influence on gastric cancer (GC) is remains to be elucidated. MicroRNAs (miRNAs/miRs) serve crucial roles in apoptosis and proliferation of cancer cells. miR-23a-3p has been shown to be associated with human GC; however, the specific function of miR-23a-3p in GC remains unclear. Therefore, the present study aimed to elucidate the role of miR-23a-3p in the regulation of GC cell proliferation and apoptosis induced *in vitro* by TSN treatment. Subsequently, apoptosis-related genes expression levels were quantified by reverse transcription-quantitative PCR and western blot analysis, respectively, and the target relationship between miR-23a-3p and *BCL2* was determined by luciferase reporter gene analysis. Additionally, cell proliferation and apoptosis experiments were carried out. The results indicated that TSN inhibited proliferation and induced apoptosis in MKN-45 cells. Moreover, it upregulated the expression of miR-23a-3p. B-cell lymphoma-2 (*BCL2*) was identified as a potential target gene of miR-23a-3p, which was demonstrated to bind to the 3'-untranslated region of *BCL2* mRNA, as detected by the luciferase reporter assay. Further studies revealed that *BCL2* expression was downregulated following overexpression of miR-23a-3p. In addition, the overexpression of the miR-23a-3p inhibited proliferation, induced G_1 arrest and increased apoptosis in MKN-45 cells. The results of the present study demonstrated that miR-23a-3p inhibited proliferation and induced apoptosis of GC cells, which may be attributable to its direct targeting of *BCL2*. These results may provide a novel insight into the apoptosis of GC cells, and may lead to investigations into the mechanisms of the effects of TSN.

Correspondence to: Professor Shuli Shao, Department of Life Science and Agroforestry, Qiqihar University, 42 Wenhua Street, JianHua, Qiqihar, Heilongjiang 161006, P.R. China
E-mail: shshl32@163.com

Key words: microRNA-23a-3p, gastric cancer, toosendanin, B-cell lymphoma 2, apoptosis

Introduction

Gastric cancer (GC) is one of the most common malignancies worldwide, ranking 5th in morbidity and 3rd in mortality among all malignancies (1,2). Surgery along with systemic chemotherapy remains the most common treatment regimen for GC. However, it has recently been observed that GC is generally refractory to conventional chemotherapy drugs (3), resulting in the poor prognosis. Thus, new chemotherapy drugs are urgently required.

Toosendanin (TSN) is a tetracyclic triterpenoid extracted from *Melia toosendan* Sieb, et Zucc, which primarily grows in specific areas of China. Previous studies indicate that TSN can induce the apoptosis of multiple human cancer cells (4,5). It has been reported that TSN induces apoptosis of AGS and HGC-27 human GC cell lines (5). Wang *et al* (6) have previously reported that TSN can induce apoptosis of human GC SGC-7901 cells partly through microRNA (miRNA/miR)-200a-mediated downregulation of the β-catenin pathway. However, the regulatory mechanisms of the effect of TSN on GC cells remain to be elucidated.

miRNAs are a class of evolutionarily conserved small single-stranded non-coding RNAs with a length of 18-25 nt that exhibit a post-transcriptional level regulatory function primarily through binding to the 3'-untranslated (3'-UTR) region of mRNAs (7,8). Several studies have reported that ~60% of human genes are regulated by different miRNAs (9,10). In addition, miRNAs directly or indirectly affect various biological processes such as cell proliferation, differentiation, apoptosis and migration (11-14). Specifically, miR-23a, has been shown to serve different roles within tumour cells (15,16). It functions as a tumour suppressor in osteosarcoma, in which its overexpression leads to reduced proliferation, migration and invasion of osteosarcoma cells (16). Additionally, miR-23a inhibits pancreatic cancer cell progression by directly targeting *polo-like kinase 1*

mRNA (17). There were 1,547 reads of hsa-miR-23a-5p detected from 115 experiments, while 3,017,274 reads of hsa-miR-23a-3p were detected from 159 experiments data from miRbase database (http://www.mirbase.org/cgi-bin/mirna_entry.pl?acc=MI0000079/, version 22.1). This indicates that the expression abundance of hsa-miR-23a-3p is much higher compared with that of hsa-miR-23a-5p, thus hsa-miR-23a-3p was selected in the present study. It was known from the miRbase database that only 1547 reads of hsa-miR-23a-5p were in the 115 experiments, while 3017274 reads of hsa-miR-23a-3p were in the 159 experiments. This indicates that the expression abundance of hsa-miR-23a-3p is many times higher than that of hsa-miR-23a-5p, so hsa-miR-23a-3p was selected. The present study found that the expression level of miR-23a-3p increased significantly in MKN-45 cells following treatment with varying concentrations of TSN. The role of miR-23a-3p, and its underlying mechanism have not been previously investigated. Thus, the present study aimed to elucidate the functions and mechanisms of miR-23a-3p in TSN-induced apoptosis of GC cells.

Materials and methods

Cell culture. The human GC cell line MKN-45 and 293T cells were purchased from the Beijing Beina Chuanglian Biotechnology Institute. MKN-45 cells were cultured in RPMI-1640 (Gibco; Thermo Fisher Scientific, Inc.), 293T cells were cultured in DMEM (Gibco; Thermo Fisher Scientific, Inc.), supplemented with 10% foetal bovine serum (Biological Industries), 100 μg/ml streptomycin, and 100 U/ml penicillin, and incubated at 37˚C in 5% CO_2 in a humidified chamber. Fluorouracil (5-FU) and 0 nmol/l TSN were used as positive control and negative control, respectively. The cells were treated with different concentrations of TSN (0, 60, 80 and 100 nmol/l) and 5-FU (80 nmol/l) for 48 h, or transfected with pcDNA3.1(+) (2 μg/ml), pcDNA3.1(+)-miR-23a-3p (2 μg/ml), miR-23a-3p inhibitor (miR-23a-3p-I; 1.0x10^{-4} mmol/l) or miR-23a-3p inhibitor-NC (miR-23a-3p-I-NC; 1.0x10^{-4} mmol/l) (Guangzhou RiboBio Co., Ltd.) using Lipofectamine® 2000 (Invitrogen; Thermo Fisher Scientific, Inc.) according to the manufacturer's instructions, then cultured for 48 h. The sequences used were as follows: miR-23a-3p-I 5'-GGAAAUCCCUGGCAAUGUGAU-3'; miR-23a-3p-I-negative control (NC) 5'-CAGUACUUUUGUGUAGUACAAA-3'. miR-23a-3p-I and miR-23a-3p-I-NC were 2'-O-methyl modified.

Cell Counting Kit-8 (CCK-8) assay for chemosensitivity. Cell survival rate and chemosensitivity were determined using a CCK-8 assay (Beyotime Institute of Biotechnology). A total of 1x10^5 MKN-45 cells were seeded in a 96-well plate. Three duplicated wells were set for each group, and the total volume of each well was 100 μl. The plate was then placed in a humidified incubator at 37˚C with 5% CO_2, and the cells were cultured for 24, 48 and 72 h with different concentrations of TSN (0, 10, 20, 30, 40, 50, 60, 70, 80, 90 and 100 nmol/l). After the indicated incubation times, 10 μl of CCK-8 was added to the plates and incubated at 37˚C for an additional 2 h. The absorbance at 450 nm was measured using a Spark 10 M multi-well plate reader (Tecan Group, Ltd.).

Vector construction. Total DNA was extracted from the MKN-45 cells using a Genomic DNA Extraction kit (centrifugal column) according to the manufacturer's instructions (BioTeke Corporation). Pre-miR-23a DNA fragment (5'-ggc cggcuggggguuccuggggaugggauuugcuuccugucacaaAUCA CAUUGCCAGGGAUUUCCaaccgacc-3') was amplified by PCR from the total DNA using Rapid PCR amplification kit according to the manufacturer's instructions (BioTeke Corporation). The PCR thermocycling conditions were as follows: Initial denaturation at 94˚C for 5 min; followed by 35 cycles of denaturation at 94˚C for 30 sec, primer annealing at 61˚C for 30 sec, extension at 72˚C for 1 min, and a final extension at 72˚C for 10 min. Then pre-miR-23a DNA fragment cloned into pcDNA3.1(+) plasmids (Promega Corporation) to construct the overexpression vector of miR-23a-3p, which was termed pcDNA3.1(+)-miR-23a-3p. The 3'-UTR of *BCL2* was PCR-amplified from MKN-45 cell genomic DNA using the same PCR protocol as the pre-miR-23a-3p and cloned into psiCHECK-2 dual-luciferase reporter plasmids (Promega Corporation) immediately downstream of the stop codon of the luciferase gene to generate psiCHECK-2-BCL2-wt. The mutant *BCL2* 3'-UTR reporter, designated as psiCHECK-2-BCL2-mu, was created by mutating the seed region of the predicted miR-23a-3p site (TATATGT to TAC ACAA) using PCR and the T-BCL primers was that used to amplify the sequence contained the mutant seed region of the predicted miR-23a-3p site (18). The primers used in plasmid construction are shown in Table I.

Acridine orange nuclear staining. Cells were cultured on glass cover slides and treated with either different concentrations of TSN (0, 60, 80 and 100 nmol/l) or transfected with pcDNA3.1(+) (2 μg/ml), pcDNA3.1(+)-miR-23a-3p (2 μg/ml), miR-23a-3p-I-NC (1.0x10^{-4} mmol/l) or miR-23a-3p-I (1.0x10^{-4} mmol/l) for 48 h. Subsequently, cells were rinsed twice with PBS and fixed with 4% paraformaldehyde in PBS for 10 min. Next, the cells were stained with 0.1 mg/ml acridine orange (Beijing Dingguo Changsheng Biotechnology Co., Ltd.) for 1-2 min. The images were captured using a Leica TCS SP8 confocal laser-scanning microscope (Leica Microsystems GmbH) at 488 nm excitation and 515 nm emission wavelengths (magnification, x63).

Cell cycle analysis. Cells were cultured to the logarithmic phase of growth in a cell culture flask and treated with different concentrations of TSN (0, 60, 80 and 100 nmol/l) or transfected with pcDNA3.1(+), pcDNA3.1(+)-miR-23a-3p (2 μg/ml), miR-23a-3p-I-NC or miR-23a-3p-I (1.0x10^{-4} mmol/l) for 48 h. The cells were then collected and centrifuged at 300 x g at 4˚C for 5 min. The pellet was resuspended in PBS and centrifuged again using the same conditions. Next, the pellet was resuspended in ice-cold 70% ethanol and stored at 4˚C for 18 h. Fixed cells were then washed with PBS and incubated in 0.5 ml staining solution [0.1 mg/ml RNase A and 0.05 mg/ml propidium iodide (PI)] at 37˚C in the dark for 30 min. The cell cycles were determined on a Cytomics FC 500 flow cytometer and CXP software 2.3 (Beckman Coulter, Inc.).

Apoptosis assay. Cells were cultured to the logarithmic phase in a cell culture flask and treated with different concentrations of

Table I. Primers for *BCL2* mRNA 3'-UTR plasmid construction.

Gene	Primer sequences (5'→3')
Pre-miR-23a F	CGGGGTACCGGGAGGTGTCCCCAAATCTCATTAC
Pre-miR-23a R	CCGGAATTCGAACTTAGCCACTGTGAACACGACT
BCL2-3'UTR F	CCGCTCGAGTCAAACAAGACGCCAACA
BCL2-3'UTR R	AAGGAAAAAAGCGGCCGCTAACAGCCACTGCCTTAAAAGTAC
mu-BCL2-3'UTR F	AACAAATAGTTTATAATACACTACTTAAACTCTAATTAATTCC
mu-BCL23'UTR R	TTAGGATAAGTTCAATTACAAATA

UTR, untranslated region; F, forward; R, reverse; mu, mutant.

TSN (0, 60, 80 and 100 nM) or transfected with pcDNA3.1(+), pcDNA3.1(+)-miR-23a-3p (2 μg/ml), miR-23a-3p-I-NC or miR-23a-3p-I ($1.0x10^{-4}$ mmol/l) for 48 h. The cells were collected, washed twice with cold PBS and 500 μl binding buffer was added to each sample. The cells were then stained with 5 μl annexin V-FITC and 5 μl PI for 15 min. The cells were immediately analysed by FC 500 flow cytometer and CXP software 2.3 (Beckman Coulter, Inc.) to determine the rate of apoptosis.

Mitochondrial membrane potential (MMP) assay. MMP was measured by flow cytometry using JC-1 (Nanjing KGI Biological Technology Development Co., Ltd.,) staining. Briefly, transfected cells were incubated with 500 μl diluted JC-1 (10 μg/ml) reagent at 37˚C in the dark for 20 min. After incubation, cells were washed with PBS and analysed within 30 min using FC 500 flow cytometer and CXP software 2.3 (Beckman Coulter, Inc.). If the mitochondrial membrane potential is high, JC-1 is gathered in the mitochondrial matrix and the formation of polymer (J-aggregates) produces red fluorescence; When the mitochondrial membrane potential is low, JC-1 cannot be concentrated in the mitochondrial matrix. Then JC-1 is a monomer and produces green fluorescence. Thus it is convenient to detect the change of mitochondrial membrane potential by the change of fluorescent color.

Reverse transcription-quantitative PCR (RT-qPCR). MKN-45 cells were seeded in 6-well plates ($1.0x10^5$ cells/well) and treated with different concentrations of TSN (0, 60, 80 and 100 nmol/l) or transfected with pcDNA3.1(+), pcDNA3.1(+)-miR-23a-3p (2 μg/ml), miR-23a-3p-I-NC, or miR-23a-3p-I ($1.0x10^{-4}$ mmol/l) for 48 h. Total RNA was extracted based on the TRIzol® method (Invitrogen; Thermo Fisher Scientific, Inc.). The concentrations of total RNA were determined spectrophotometrically using a NanoDrop 2000C Spectrophotometer (Thermo Fisher Scientific, Inc.). A first-strand cDNA was synthesized with 1μg of total RNA from each sample using a TransScriptROne-Step gDNA Removal and cDNA Synthesis Super Mix (Beijing TransGen Biotech Co., Ltd) according to the manufacturer's instructions. 2X Plus SYBR Real-time PCR mixture (BioTeke Corporation) was used for qPCR. The thermocycling conditions were as follows: 95˚C for 2 min, followed by 40 cycles of 95˚C for 15 sec, and 60˚C for 30 sec. miRNAs are short and have no ploy (A) structure, so stem-loop RT-PCR was used to detect the miRNA expression (19). The expression of human *β-actin* or *U6* was used as an internal control for mRNA or miRNA expression levels, respectively, and the relative expression level was measured by the $2^{-\Delta\Delta Cq}$ method (20). Primers used are detailed in Table II.

Western blot analysis. MKN-45 cells were seeded in 6-well plates ($1.0x10^5$ cells/well) and treated with different concentrations of TSN (0, 60, 80 and 100 nmol/l) or transfected with pcDNA3.1(+) (2 μg/ml), pcDNA3.1(+)-miR-23a-3p (2 μg/ml), miR-23a-3p-I-NC ($1.0x10^{-4}$ mmol/l), or miR-23a-3p-I ($1.0x10^{-4}$ mmol/l) for 48 h. Cells were harvested and lysed in RIPA buffer containing a protease inhibitor cocktail (Beyotime Institute of Biotechnology). The lysate was centrifuged at 12,000 x g for 10 min at 4˚C. The supernatant was then collected, and the protein concentration was determined using the BCA Protein Assay Kit (Beyotime Institute of Biotechnology). The same protein amounts (10 μg in each lane) were loaded and separated by 10% SDS-PAGE, followed by transfer to polyvinylidene fluoride membranes (EMD Millipore) using the western blotting apparatus. The membranes were blocked with 5% (w/v) fat-free milk in Tris-buffered saline containing 0.05% Tween-20 (TBS-T) and then incubated with primary antibodies at 4˚C overnight. Membranes were probed with the following primary antibodies (all 1:300): Anti-BCL2 polyclonal (cat. no. ab196495; Abcam), anti-Bax polyclonal (cat. no. ab53154; Abcam), anti-active caspase-3 monoclonal (cat. no. bsm-33284M; BIOSS), anti-caspase-8 polyclonal (cat. no. bs-0052R; BIOSS), anti-caspase-9 polyclonal (cat. no. bs-0049R; BIOSS), anti-cytochrome *c* polyclonal (cat. no. bs-0013R; BIOSS), anti-Fas polyclonal (cat. no. bs-6477R; BIOSS), anti-apoptotic protease activating factor 1 polyclonal (cat. no. ab2000; Abcam) and anti-β actin polyclonal (cat. no. ab8227; Abcam). The membranes were subsequently incubated with IRDye 800CW® goat anti-rabbit (926-32211) and IRDye 800CW® goat anti-mouse (926-32210) secondary antibody (1:15,000; LI-COR Biosciences) for 90 min at 20-25˚C and washed with PBS. The bands were visualized and quantified using the Li-COR Odyssey infrared imaging system (Li-COR Biosciences); each band was normalised to its respective β-actin band.

Dual-luciferase reporter assay. To explore the mechanisms of miR-23a-3p-induced apoptosis, the target genes of mir-23a-3p were predicted by TargetScan websites (TargetScan: https://www.targetscan.org, version 7.1) (21) and examined by luciferase reporter assay. 293T cells ($2x10^4$ cells/well) were plated in a

Table II. Primers for RT-qPCR.

Gene	RT primer (5'→3')	qPCR primer sequences	
		Forward (5'→3')	Reverse (5'→3')
miR-23a-3p	CTCAACTGGTGTCGTGGAGTCG GCAATTCAGTTGAGGGAAATCC	ACACTCCAGCTGGGATCA CATTGCCAGGGAT	CTCAACTGGTGTCGT GGA
miR-148	CTCAACTGGTGTCGTGGAGTCGG CAATTCAGTTGAGAGTTCGGAG	ACACTTCCAGCTGGGAA AGTTGAGACACTC	CTCAACTGGTGTCGT GGA
miR-34a-5p	CTCAACTGGTGTCGTGGAGTCGG CAATTCAGTTGAGACAACCAG	ACACTCCAGCTGGGTGG CAGTGTCTTAGCTGG	CTCAACTGGTGTCGT GGA
miR-365a-3p	CTCAACTGGTGTCGTGGAGTCG GCAATTCAGTTGAGATAAGGAT	ACACTCCAGCTGGGTAA TGCCCCTAAAAATCC	CTCAACTGGTGTCGT GGA
BCL2		ATGTGTGTGAGAGCGTC AAC	AGACAGCCAGGAGA AATCAAAC
Bax		AAGCTGAGCGAGTGTATC AAG	CAAAGTAGAAAAGG GCGACAAC
Fas		TGATGTGGAACACAGCA AGG	GGCTGTGGTGACTCT TAGTGATAA
Cyt *c*		CTGGGTGACGAGTGAAA CTG	TGAGCACAACAGGA ACTGGA
Caspase-3		GGAACGAACGGACCT GTG	GCCTCCACTGGTAT CTTCTG
Caspase-8		GAGACAAGGGCATCATC TACGGC	TGGGTTTACCACGAA GGGAAGG
Caspase-9		GGACATCCAGCGGGC AGG	TCTAAGCAGGAGATG AACAAAGG
APAF-1		AAGGTGGAGTACCACA GAG	TCCATGTATGGTGAC CCATCC
β-actin		AGCGAGCATCCCCCAAA GTT	GGGCACGAAGGCTC ATCATT
U6		CTCGCTTCGGCAGCACA	AACGCTTCACGAATT TGCGT

qPCR, quantitative PCR; APAF, apoptotic protease activating factor 1; Cyt *c*, cytochrome *c*; RT, reverse transcription; miR, microRNA.

24-well plate (Corning, Inc.) 24 h before transfection. Cells were co-transfected with 0.5 μg of either the psiCHECK-2-BCL2-wt, psiCHECK-2-BCL2-mu or empty vector psiCHECK-2, and either pcDNA3.1(+) (2 μg/ml), pcDNA3.1(+)-miR-23a-3p (2 μg/ml), miR-23a-3p-I-NC ($1x10^{-4}$ mmol/l) or miR-23a-3p-I ($1x10^{-4}$ mmol/l) using Lipofectamine® 2000 (Invitrogen; Thermo Fisher Scientific, Inc.) according to the manufacturer's instructions. After 48 h of transfection, cells were lysed in Passive Lysis Buffer (Promega Corporation), and the activities of the firefly and Renilla luciferase were measured with a GloMax 20/20 Luminometer (Promega Corporation) using the Dual-Luciferase Reporter Assay System according to the manufacturer's protocols. Transfections were performed in duplicate and were repeated three times.

Statistical analysis. All the results were expressed as mean ± SEM. All statistical analyses and graphing were performed using SPSS 17.0 software (SPSS, Inc.) and GraphPad Prism 5.0 software (GraphPad Software, Inc.), respectively. Statistical differences were determined using one-way ANOVA followed by a Tukey's post hoc test. $P<0.05$ was considered to indicate a statistically significant difference.

Results

TSN inhibits proliferation and induces apoptosis in MKN-45 cells. CCK-8 and cell cycle assays were carried out to evaluate the effect of TSN on MKN-45 cell proliferation. The results showed that inhibitory rates on MKN-45 cells treated with TSN significantly increased as the rise of TSN concentration and prolongation of time, (Fig. 1A), the IC_{50} value was 81.06 nmol/l for 48 h, and the cell cycle was arrested at the G1 phase with increasing concentrations of TSN compared with the negative control (Fig. 1B and C). Compared with those in the negative control, the TSN-treated cells showed the cell nucleus cleavage and chromatin morphological changes. Acridine orange staining revealed a higher number of apoptotic bodies following the addition of TSN (Fig. 2A), and flow cytometry demonstrated that the early apoptotic rates gradually increased (Fig. 2B and C). Moreover, compared with

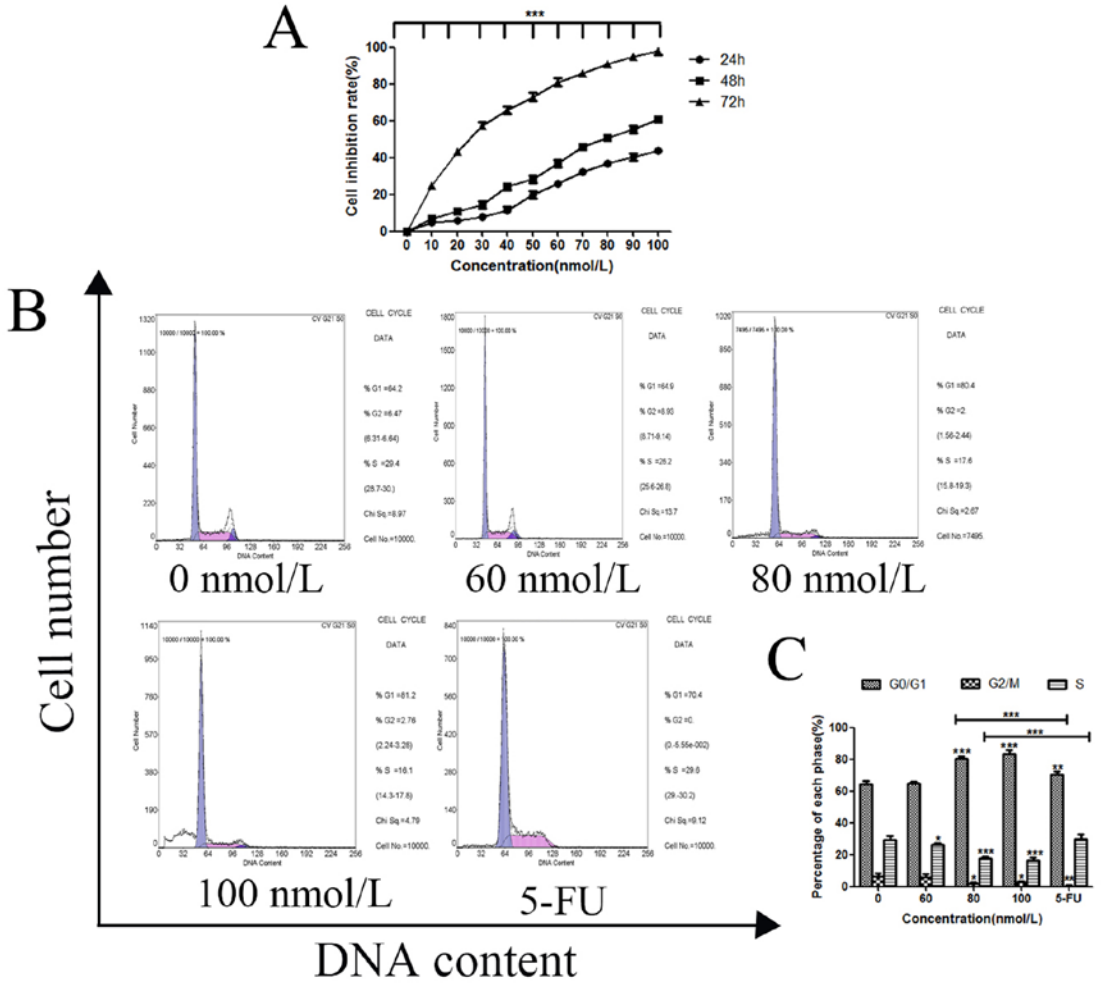

Figure 1. Cytotoxic effects of TSN on MKN-45 cells. (A) MKN-45 cells were seeded into 96-well plates and treated with varying concentrations of TSN for 24, 48 and 72 h. The growth inhibition effects of TSN were determined by Cell Counting Kit-8 assay. (B and C) The cell cycle of MKN-45 cells was analysed by flow cytometry after treatment with varying concentrations of TSN for 48 h. All results are expressed as the mean ± SEM of three independent experiments; n=3; *P<0.05, **P<0.01, ***P<0.001 vs. 0 nM or as indicated. TSN, toosendanin.

the negative control, the mRNA and protein expression levels of Bax, cytochrome *c*, Fas, caspase-3, caspase-8, caspase-9 and APAF-1 were significantly upregulated, reaching the maximum at 80 nmol/l concentration of TSN, and decreasing following the addition of 100 nmol/l (Fig. 2D-F). However, the expression of *BCL2* was significantly downregulated at 80 nmol/l TSN, and increased following the addition of 100 nmol/l, which suggested that TSN may also activate other mechanisms to inhibit the proliferation of gastric cancer cells at 100 nmol/l. The effect in the 80 nmol/l TSN treatment group was more evident compared with the 5-FU treatment group.

TSN suppresses the expression of BCL2 partly through upregulation of miR-23a-3p. BCL2 is an integral mitochondrial membrane protein and acts as a switch to control the process of mitochondrial pathway apoptosis (22,23). As shown in Fig. 2D-F, the expression of BCL2 was significantly downregulated in MKN-45 cells following treatment with TSN. To explore the apoptotic mechanism employed by TSN, miRNAs targeting *BCL2* were predicted (Fig. 3A), and the expression of these miRNAs was evaluated using RT-qPCR in MKN-45 cells following treatment with different concentrations of TSN for 48 h. After TSN treatment, the expression levels of miR-23a-3p, miR-34a-5p and miR-365a-3p were markedly increased compared with the negative control; however, a similar change was not observed in miR-148a-5p expression (Fig. 3B). It was found that the expression of miR-23a-3p increased significantly upon increasing TSN concentration and reached a maximum when the TSN concentration was increased to 80 nmol/l. Since the expression level of miR-23a-3p was the more significant, the study focused on miR-23a-3p for the subsequent experiments.

To validate whether *BCL2* was the direct target genes of miR-23a-3p, a dual-luciferase reporter system was employed. 3'UTR sequences containing the predicted target site of miR-23a-3p or mutated sequences were cloned into the psiCHECK-2, respectively. Co-transfection of pcDNA3.1 (+)-miR-23a-3p with psiCHECK-2-BCL2-wt in 293T cells showed that luciferase activity was significantly lower than those of controls (P<0.001) (Fig. 3C). Co-transfection pcDNA3.1 (+)-miR-23a-3p with psiCHECK-2- BCL2-mu did not change the luciferase activities (P>0.05) (Fig. 3C).

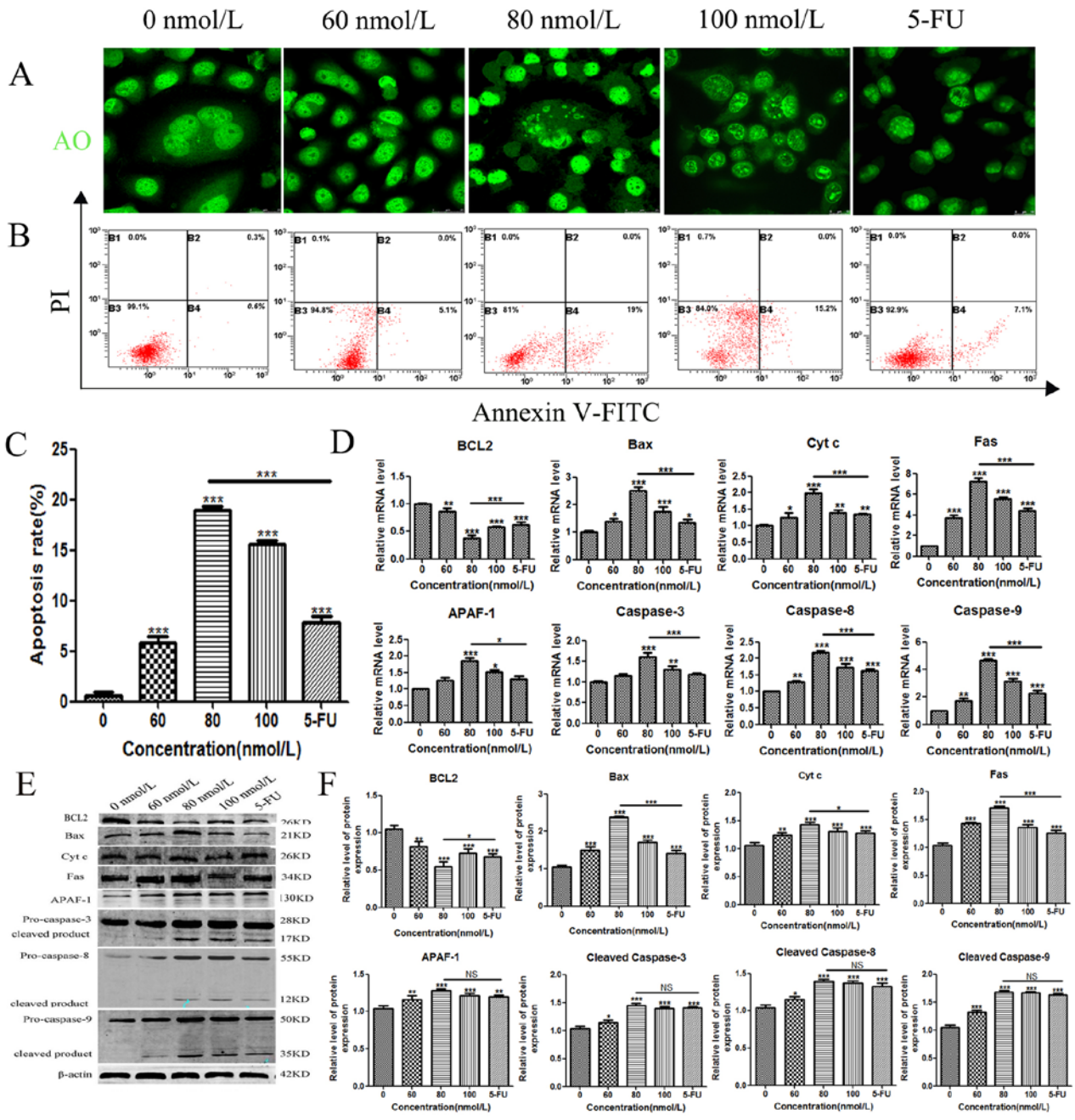

Figure 2. Apoptotic effects of TSN on MKN-45 cells. (A) MKN-45 cells were seeded into 6-well plates and treated with varying concentrations of TSN for 48 h, incubated with acridine orange, and visualised using laser confocal microscope. (B and C) Early apoptotic effects of TSN were evaluated by flow cytometry analysis after staining with annexin V-FITC and PI. (D) The mRNA expression of *Caspase-3*, *8*, *9*, *BAX*, *BCL2*, *FAS*, Cyt *c* and *APAF1* was detected using reverse transcription quantitative PCR in TSN-treated MKN-45 cells. (E and F) Protein expression levels of Caspase-3, 8, 9, Bax, BCL2, Fas, Cyt *c* and APAF-1 were detected using western blotting in TSN-treated MKN-45 cells. β-actin was used as an internal control. All results are expressed as the mean ± SEM of three independent experiments; n=3; *P<0.05, **P<0.01, ***P<0.001 vs. 0 nM. Cyt *c*, cytochrome *c*; TSN, toosendanin; APAF1, apoptotic protease activating factor 1; 5-FU, fluorouracil.

Compared with miR-23a-3p-I-NC, miR-23a-3p-I abolished the targeting 3'UTR of *BCL2* (Fig. 3D). This finding suggested that miR-23a-3p may directly target the 3'-UTR of the *BCL2* mRNA. Based on this evidence, whether miR-23a-3p regulated the expression of *BCL2* in MKN-45 cells was examined. Endogenous mRNA and protein expression levels of BCL2 were markedly downregulated following overexpression of miR-23a-3p and upregulated following the silencing of miR-23a-3p with the inhibitor (Fig. 3E-H).

miR-23a-3p induces MKN-45 apoptosis. To identify the effects of miR-23a-3p on apoptosis in MKN-45 cells, a series of cell apoptosis experiments were performed. Compared with those in the pcDNA3.1(+) group, cells transfected with pcDNA3.1(+)-miR-23a-3p exhibited more pronounced nuclear morphology changes, which included the appearance of concentrated, agglomerated and marginalised chromatin as well as a small number of nuclei becoming ruptured (Fig. 4A). By contrast, compared with cells in

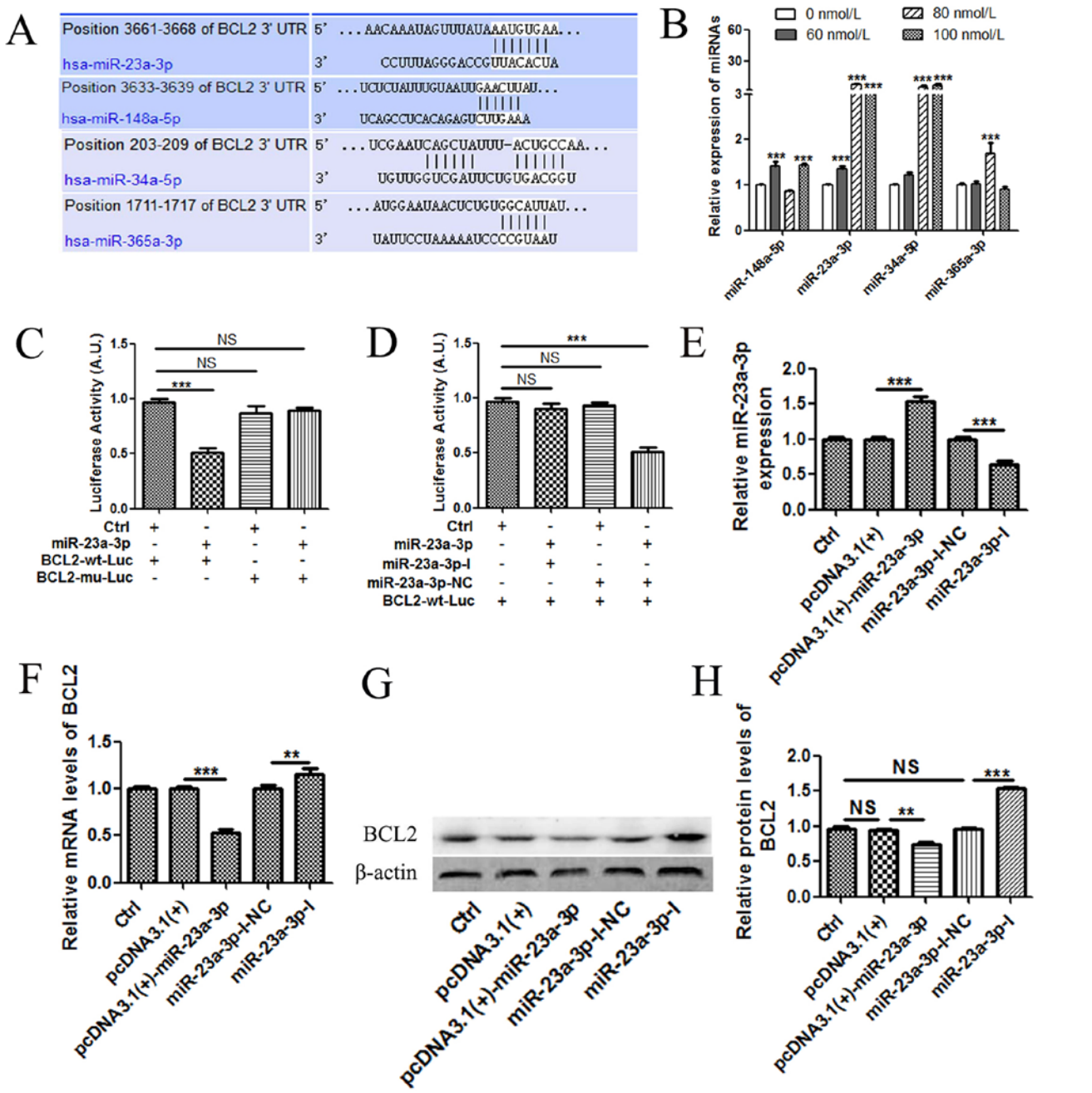

Figure 3. TSN upregulates the expression of miR-23a-3p, which subsequently downregulates the expression of *BCL2*. (A) As predicted in the TargetScan database, the *BCL2* 3'-UTR contained several potential miRNA binding sites. (B) MKN-45 cells were treated with varying concentrations of TSN for 48 h, and the changes in miRNA expression levels were detected by RT-qPCR. (C) miR-23a-3p significantly inhibited the luciferase activities. (D) miR-23a-3p inhibitors abolished the targeting 3'UTR of *BCL2*. (E) The expression of miR-23a-3p in MKN-45 cells after transfection with pcDNA3.1(+), pcDNA3.1(+)-miR-23a-3p, miR-23a-3p-I-NC or miR-23a-3p-I. The expression of *BCL2* mRNA was determined by (F) RT-qPCR and (G and H) western blot analysis. All results are expressed as the mean ± SEM of three independent experiments; n=3; **P<0.01, ***P<0.001. Ctrl, control; miR, microRNA; RT-qPCR, reverse transcription-quantitative PCR; UTR, untranslated region; mu, mutant; wt, wild-type; luc, luciferase; NC, negative control; NS, not significant; miR, microRNA; I, inhibitor; TSN, toosendanin.

the miR-23a-3p-I-NC group, the nuclei transfected with miR-23a-3p-I were intact. Subsequently, annexin V-FITC/PI double staining assay was performed to detect apoptosis in transfected MKN-45 cells (Fig. 4B and C). The results indicated that the early apoptotic rate of cells transfected with pcDNA3.1(+)-miR-23a-3p was significantly higher compared with that of cells transfected with pcDNA3.1(+) for 48 h. By contrast, the rate of apoptosis of cells transfected with miR-23a-3p-I was lower compared with that of cells transfected with miR-23a-3p-I-NC.

The changes in MMP were determined by flow cytometry (Fig. 4D and E). Following transfection with pcDNA3.1(+)-miR-23a-3p, MMP was decreased in MKN-45 cells compared with its level in cells transfected with pcDNA3.1(+). However, the MMP was increased in cells transfected with miR-23a-3p-I compared with the NC cells

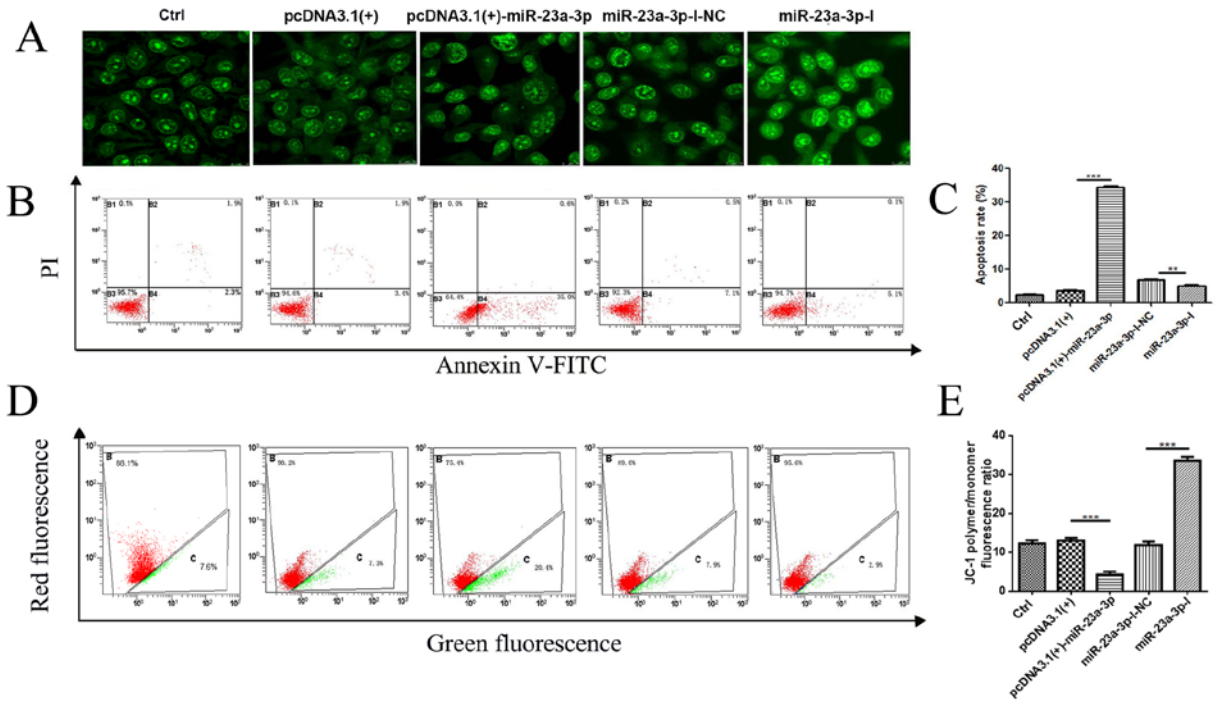

Figure 4. miR-23a-3p induces apoptosis of MKN-45 cells. MKN-45 cells were transfected with pcDNA3.1(+), pcDNA3.1(+)-miR-23a-3p, miR-23a-3p-I-NC or miR-23a-3p-I for 48 h. (A) Morphological changes in MKN-45 cells nuclei, observed after acridine orange staining. The images were obtained with a Leica SP8 and analysed under HCX PL APO CS (magnification, 63x). (B and C) The early apoptotic rates of transfected MKN-45 cells were investigated by flow cytometry analysis using annexin V-FITC and PI double labelling. (D and E) Mitochondrial membrane potential changes in MKN-45 cells were determined by JC-1 staining. Red channels: JC-1 polymer; Green channels: JC-1 monomer. All results are expressed as the mean ± SEM of three independent experiments; n=3; **P<0.01, ***P<0.001. miR, microRNA; I, inhibitor; NC, negative control; Ctrl, control; MMP; PI, propidium iodide.

transfected with miR-23a-3p-I-NC. These findings indicated that miR-23a-3p may induce apoptosis in MKN-45 cells.

miR-23a-3p arrests cell cycle in MKN-45 cells. To identify the effects of miR-23a-3p on cell cycle distribution, a cell cycle study was conducted in MKN-45 cells by PI single staining (Fig. 5A and B). Compared with pcDNA3.1(+), the number of cells in the G_1/G_0 phase of MKN-45 cells increased significantly after transfection with pcDNA3.1(+)-miR-23a-3p, and the number of cells in the S phase decreased significantly, resulting in inhibition of cell proliferation in the G_1 phase after transfection. Conversely, compared with that in the miR-23a-3p-I-NC group, the number of cells in the G_1/G_0 phase of MKN-45 cells decreased, whereas the number in the S phase increased after transfection with miR-23a-3p-I. These results indicated that the cycle became arrested in the G_1 phase following overexpression of miR-23a-3p in MKN-45 cells.

Discussion

TSN has been regarded as an effective drug to induce apoptosis of tumor cells (24). TSN has been reported to inhibit proliferation and induce apoptosis in human colorectal cancer (25) and hepatocarcinoma cells (26). However, the exact functions and mechanisms of the apoptotic effects of TSN on human GC cells remain largely unclear. In the present study, the results demonstrated that TSN inhibited proliferation and induced apoptosis in MKN-45 cells. Previous studies have reported that TSN inhibits a number of pathways and targets that are crucial to cancer cell survival and proliferation (4), such as TSN induced apoptosis of cells through the β-catenin and MAPK pathways (6,5). Zhang *et al* (27) has previously shown that TSN selectively inhibits U87 and C6 glioma cell proliferation and induces apoptosis through oestrogen receptor-dependent machinery. In order to study the mechanism of TSN-induced apoptosis of human gastric cancer MKN-45 cells, the expression of apoptosis-related genes was examined. The expression of these genes (cytochrome *c*, *Fas*, *caspase-3*, *caspase-8*, *caspase-9* and *APAF-1*) increased with the increase of TSN concentration. In addition, toosendanin was found to upregulate the expression of Bax and downregulate the expression of Bcl-2, altering the Bax/Bcl-2 ratio.

Apoptosis is a complex process involving several genes and miRNAs (28). However, which miRNAs are involved in TSN-induced apoptosis of gastric cancer cells remains to be elucidated. The present study found that the expression of miR-23a-3p increased significantly with the increase in TSN concentration. This is similar to the results of Zhao *et al* (29), who found that mir-148a inhibits cell proliferation and promotes paclitaxel-induced apoptosis of ovarian cancer cells.

miR-23a has been reported to be associated with human GC (30). However, the role of miR-23a-3p in GC, along with its underlying mechanisms, remains to be fully elucidated. The present study demonstrated that overexpression of miR-23a-3p significantly inhibited proliferation and induced the apoptosis of GC cells, whereas inhibition of miR-23a-3p had the opposite effects. Therefore, miR-23a-3p may be a key target for the induction of apoptosis in GC cells. However, the effects of miR-23a

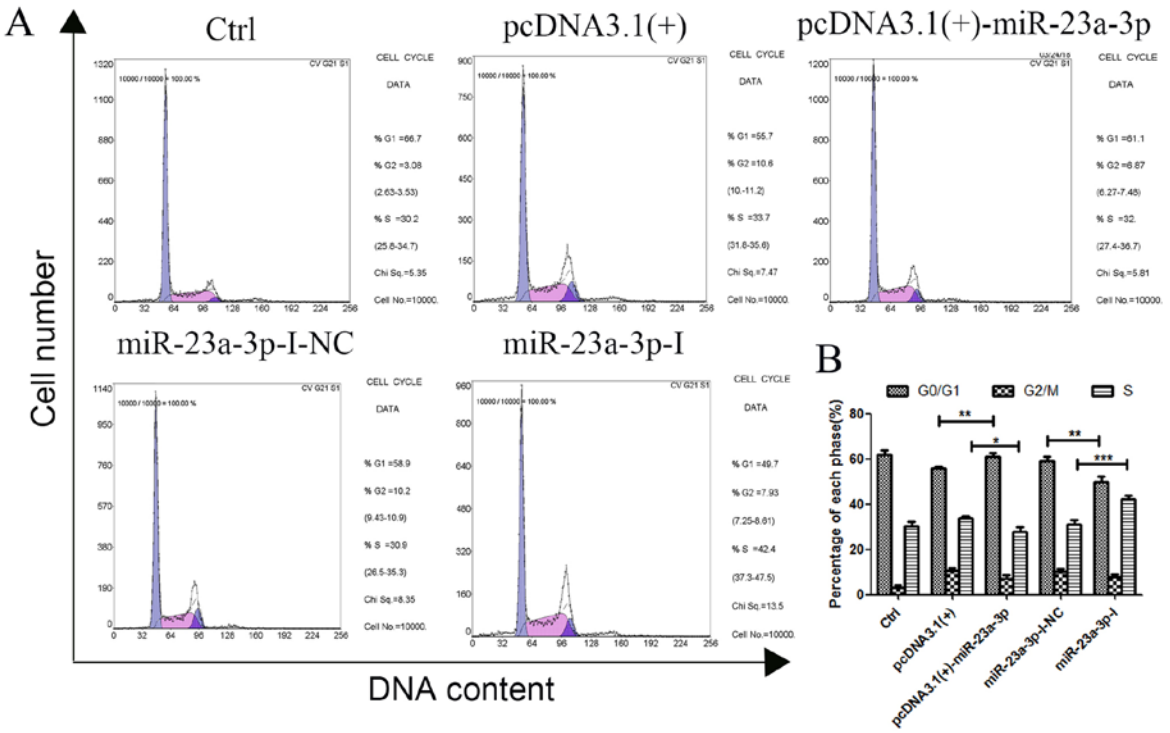

Figure 5. miR-23a-3p suppresses MKN-45 cell cycle progression. (A and B) The cell cycle of MKN-45 cells was analysed by flow cytometry following transfection with pcDNA3.1(+), pcDNA3.1(+)-miR-23a-3p, miR-23a-3p-I-NC or miR-23a-3p-I for 48 h. All results are expressed as the mean ± SEM of three independent experiments; n=3; *P<0.05, **P<0.01, ***P<0.001. miR, microRNA; I, inhibitor; NC, negative control; CK, control.

on cancer cell proliferation remain controversial. For example, miR-23a is known to suppress the proliferation of osteosarcoma cells by targeting special AT-rich sequence-binding protein-1 (31) but promotes colorectal cancer cell survival by targeting *PDK4* (32). Collectively, these findings suggest that the function of miR-23a in cancer cells differs by targeting different genes. However, the genes targeted by miR-23a-3p to induce apoptosis in GC cells remain to be clarified. In this study, an inverse correlation was noted between the expression of miR-23a-3p and *BCL2* in GC cells, suggesting that miR-23a-3p may be involved in the apoptosis of MKN-45 cells.

BCL2 is an essential mitochondrial membrane protein and is regulated by a number of miRNAs (33). Liao *et al* (34) reported that miRNA-448 inhibits cell growth by targeting *BCL2* in hepatocellular carcinoma. Chen *et al* (35) reported that miRNA-449a is downregulated in osteosarcoma and promotes cell apoptosis by targeting *BCL2*. In the present study, *BCL2* was identified as a target gene of miR-23a-3p, and miR-23a-3p was able to downregulate the mRNA and protein expression levels of BCL2 by binding directly to the 3'-UTR of *BCL2* mRNA in MKN-45 GC cells.

In this study, the expression level of miR-34a-5p also increased significantly after TSN treatment, which suggested that miR-34a-5p may also be involved in the regulation of TSN-induced apoptosis of GC cells. However, whether miR-34a-5p is involved in TSN-induced apoptosis requires further study. In the future more work to intensify this research in other GC cell lines is needed, so that we can better improve the mechanism of TSN-induced apoptosis; meanwhile future studies are also required to explore whether miR-23a has any effect on the migration and invasion of GC cells.

In conclusion, the present study demonstrated that TSN induces apoptosis of MKN-45 cells in part through the miR-23a-3p/*BCL2* axis. These results may provide novel insights into the growth of GC cells. Further studies identifying additional mechanisms of TSN will be interesting to pursue.

Acknowledgements

Not applicable.

Funding

This work was supported by the National Natural Science Foundation of China (grant number no. 31670843), the Natural Science Foundation of Heilongjiang Province, China (grant nos. C2016057 and C201241), the Scientific Research Fund of Heilongjiang Provincial Education Department (grant nos. 135109104 and 135209260), and the Basic scientific research Fund of Heilongjiang Provincial institutions of university (grant nos. STSXK201809 and LTSW201737).

Availability of data and materials

All data generated or analysed during this study are included in this published article.

Authors' contributions

SL performed data analysis and drafted the manuscript. CL, SZ, YF and YP performed data analysis and participated in intellectual discussion. WZ designed flow cytometry experiments

and assisted with critical revisions of the manuscript. ZZ captured the images using a confocal laser microscope. SS obtained funding for the study and assisted with the design and interpretation of the study, as well as critical revisions of the manuscript. All authors read and approved the final manuscript.

Ethics approval and consent to participate

Not applicable.

Patient consent for publication

Not applicable.

Competing interests

The authors declare that they have no competing interests.

References

1. Rugge M, Genta RM, Di Mario F, El-Omar EM, El-Serag HB, Fassan M, Hunt RH, Kuipers EJ, Malfertheiner P, Sugano K and Graham DY: Gastric cancer as preventable disease. Clin Gastroenterol Hepatol 15: 1833-1843, 2017.
2. Kosaka T, Endo M, Toya Y, Abiko Y, Kudara N, Inomata M, Chiba T, Takikawa Y, Suzuki K and Sugai T: Long-term outcomes of endoscopic submucosal dissection for early gastric cancer: A single-center retrospective study. Dig Endosc 26: 183-191, 2014.
3. Ilson DH: Advances in the treatment of gastric cancer. Curr Opin Gastroenterol 34: 465-468, 2018.
4. Gao T, Xie A, Liu X, Zhan H, Zeng J, Dai M and Zhang B: Toosendanin induces the apoptosis of human Ewing's sarcoma cells via the mitochondrial apoptotic pathway. Mol Med Rep 20: 135-140, 2019.
5. Zhou Q, Wu X, Wen C, Wang H, Wang H, Liu H and Peng J: Toosendanin induces caspase-dependent apoptosis through the p38 MAPK pathway in human gastric cancer cells. Biochem Biophys Res Commun 505: 261-266, 2018.
6. Wang G, Huang Y, Zhang R, Hou L, Liu H, Chen X, Zhu J and Zhang J: Toosendanin suppresses oncogenic phenotypes of human gastric carcinoma SGC-7901 cells partly via miR-200a-mediated downregulation of β-catenin pathway. Int J Oncol 51: 1563-1573, 2017.
7. Adams BD, Parsons C, Walker L, Zhang WC and Slack FJ: Targeting noncoding RNAs in disease. J Clin Invest 127: 761-771, 2017.
8. Wu HH, Lin WC and Tsai KW: Advances in molecular biomarkers for gastric cancer: miRNAs as emerging novel cancer markers. Expert Rev Mol Med 16: e1, 2014.
9. Wang J, Wang Q, Liu H, Hu B, Zhou W and Cheng Y: MicroRNA expression and its implication for the diagnosis and therapeutic strategies of gastric cancer. Cancer Lett 297: 137-143, 2010.
10. Han R, Chen X, Li Y, Zhang S, Li R and Lu L: MicroRNA-34a suppresses aggressiveness of hepatocellular carcinoma by modulating E2F1, E2F3, and Caspase-3. Cancer Manag Res 11: 2963-2976, 2019.
11. Yang T, Zeng H, Chen W, Zheng R, Zhang Y, Li Z, Qi J, Wang M, Chen T, Lou J, *et al*: Helicobacter pylori infection, H19 and LINC00152 expression in serum and risk of gastric cancer in a Chinese population. Cancer Epidemiol 44: 147-153, 2016.
12. Wang Y, Melton C, Li Y, Shenoy A, Zhang X, Subramanyam D and Blelloch R: miR-294/miR-302 promotes proliferation, suppresses G1-S restriction point, and inhibits ESC differentiation through separable mechanisms. Cell Rep 4: 99-109, 2013.
13. Liu XH, Lu KH, Wang KM, Sun M, Zhang EB, Yang JS, Yin DD, Liu ZL, Zhou J, Liu ZJ, *et al*: MicroRNA-196a promotes non-small cell lung cancer cell proliferation and invasion through targeting HOXA5. BMC Cancer 12: 348, 2012.
14. Ding F, Lai J, Gao Y, Wang G, Shang J, Zhang D and Zheng S: NEAT1/miR-23a-3p/KLF3: A novel regulatory axis in melanoma cancer progression. Cancer Cell Int 19: 217, 2019.
15. Liu P, Wang C, Ma C, Wu Q, Zhang W and Lao G: MicroRNA-23a regulates epithelial-to-mesenchymal transition in endometrial endometrioid adenocarcinoma by targeting SMAD3. Cancer Cell Int 16: 67, 2016.
16. He Y, Meng C, Shao Z, Wang H and Yang S: MiR-23a functions as a tumor suppressor in osteosarcoma. Cell Physiol Biochem 34: 1485-1496, 2014.
17. Chen B, Zhu A, Tian L, Xin Y, Liu X, Peng Y, Zhang J, Miao Y and Wei J: miR23a suppresses pancreatic cancer cell progression by inhibiting PLK1 expression. Mol Med Rep 18: 105-112, 2018.
18. Rigotto C, Sincero TC, Simões CM and Barardi CR: Detection of adenoviruses in shellfish by means of conventional-PCR, nested-PCR, and integrated cell culture PCR (ICC/PCR). Water Res 39: 297-304, 2005.
19. Chen C, Ridzon DA, Broomer KJ, Zhou ZH, Lee DH, Nguyen JT, Barbisin N, Xu LN, Mahuvakar VR, Andersen MR, *et al*: Real-time quantification of microRNAs by stem-loop RT-PCR. Nucleic Acids Res 33: e179, 2005.
20. Livak KJ and Schmittgen TD: Analysis of relative gene expression data using real-time quantitative PCR and the 2(-Delta Delta C(T)) method. Methods 25: 402-408, 2001.
21. Sui CG, Meng FD, Li Y and Jiang YH: miR-148b reverses cisplatin-resistance in non-small cell cancer cells via negatively regulating DNA (cytosine-5)-methyltransferase 1(DNMT1) expression. J Transl Med 13: 132, 2015.
22. Schenk RL, Strasser A and Dewson G: BCL-2: Long and winding path from discovery to therapeutic target. Biochem Biophys Res Commun 482: 459-469, 2017.
23. Cory S and Adams JM: The Bcl2 family: Regulators of the cellular life-or-death switch. Nat Rev Cancer 2: 647-656, 2002.
24. Zhang T, Li J, Yin F, Lin B, Wang Z, Xu J, Wang H, Zuo D, Wang G, Hua Y and Cai Z: Toosendanin demonstrates promising antitumor efficacy in osteosarcoma by targeting STAT3. Oncogene 36: 6627-6639, 2017.
25. Wang G, Feng C, Chu S, Zhang R, Lu Y, Zhu J and Zhang J: Toosendanin inhibits growth and induces apoptosis in colorectal cancer cells through suppression of AKT/GSK-3beta/beta-catenin pathway. Int J Oncol 47: 1767-1774, 2015.
26. Liu XL, Wang H, Zhang L, Wang YL, Wang J, Wang P, He X and He YJ: Anticancer effects of crude extract from Melia toosendan Sieb. et Zucc on hepatocellular carcinoma in vitro and in vivo. Chin J Integr Med 22: 362-369, 2016.
27. Zhang S, Cao L, Wang ZR, Li Z and Ma J: Anti-cancer effect of toosendanin and its underlying mechanisms. J Asian Nat Prod Res 21: 270-283, 2019.
28. Ambros V: The functions of animal microRNAs. Nature 431: 350-355, 2004.
29. Zhao S, Wen Z, Liu S, Liu Y, Li X, Ge Y and Li S: MicroRNA-148a inhibits the proliferation and promotes the paclitaxel-induced apoptosis of ovarian cancer cells by targeting PDIA3. Mol Med Rep 12: 3923-3929, 2015.
30. Hua K, Chen YT, Chen CF, Tang YS, Huang TT, Lin YC, Yeh TS, Huang KH, Lee HC, Hsu MT, *et al*: MicroRNA-23a/27a/24-2 cluster promotes gastric cancer cell proliferation synergistically. Oncol Lett 16: 2319-2325, 2018.
31. Wang G, Li B, Fu Y, He M, Wang J, Shen P and Bai L: miR-23a suppresses proliferation of osteosarcoma cells by targeting SATB1. Tumour Biol 36: 4715-4721, 2015.
32. Deng Y, Deng Z, Hao H, Wu X, Gao H, Tang S and Tang H: MicroRNA-23a promotes colorectal cancer cell survival by targeting PDK4. Exp Cell Res 373: 171-179, 2018.
33. Weyhenmeyer B, Murphy AC, Prehn JH and Murphy BM: Targeting the anti-apoptotic Bcl-2 family members for the treatment of cancer. Exp Oncol 34: 192-199, 2012.
34. Liao ZB, Tan XL, Dong KS, Zhang HW, Chen XP, Chu L and Zhang BX: miRNA-448 inhibits cell growth by targeting BCL-2 in hepatocellular carcinoma. Dig Liver Dis 51: 703-711, 2019.
35. Chen J, Zhou J, Chen X, Yang B, Wang D, Yang P, He X and Li H: miRNA-449a is downregulated in osteosarcoma and promotes cell apoptosis by targeting BCL2. Tumour Biol 36: 8221-8229, 2015.